



Characteristics of slow pyrolysis biochars produced from rhodes grass and fronds of edible date palm



Mustapha Jouiad^{a,*}, Naeema Al-Nofeli^b, Nahid Khalifa^b,
Farah Benyettou^c, Lina F. Yousef^{b,*}

^a Masdar Institute of Science and Technology, Institute Center for Energy (iENERGY), Abu Dhabi, United Arab Emirates

^b Masdar Institute of Science and Technology, Institute Center for Water and Environment (iWATER), Abu Dhabi, United Arab Emirates

^c New York University Abu Dhabi, Center of Science and Engineering, Abu Dhabi, United Arab Emirates

ARTICLE INFO

Article history:

Received 31 July 2014

Accepted 31 October 2014

Available online 26 November 2014

Keywords:

Biomass

FTIR

Lignocellulose

SEM

TGA

Water sorption

ABSTRACT

Biochars from two different biomass (rhodes grass and fronds of date palm) were produced using the same pyrolysis condition (1 atm, 400 °C, heating rate of 5 °C min⁻¹, duration of 11 h) and compared in terms of chemical composition, thermal stability, and respective microstructures. Proximate analysis of the biochars showed rhodes grass has higher fixed carbon (56.6 wt%), lower volatile (11.8 wt%) and higher ash (28.8 wt%) compared to date palm biochar (fixed carbon 45 wt%; volatile 43.2 wt%; ash 7.1 wt%). The pH of the two biochars were similar (~9.6). Elemental analysis showed that carbon becomes enriched, whereas hydrogen, oxygen and sulfur become depleted after pyrolysis. The elemental O/C and (O + N)/C ratios are lower in rhodes grass biochar (0.11 and 0.12 respectively) compared to date palm biochar (0.32 and 0.33 respectively), but both biochars have a similar H/C ratio (0.46 for rhodes grass and 0.49 for date palm). Thermogravimetric Analysis (TGA) performed in inert gas (N₂) showed considerable differences in the thermal degradation profile of the two biochars. Only one degradation event occurring over a wide temperature range (120–1000 °C; no obvious degradation maximum) was observed in rhodes grass, whereas two degradation events were observed in date palm – the first occurring rapidly (280–380 °C; maximum at 340 °C) and the second event occurring slowly over a wider temperature range (380–1000 °C; no temperature maximum detected). The Fourier transform infrared (FTIR) spectra of both biochars are featureless in comparison to raw biomass, but bands assigned to O–H stretching (3200–3000 cm⁻¹) and C–H stretching (3100–3000 cm⁻¹) while markedly decreased suggest cellulose might not have been completely decomposed during pyrolysis. The BET surface area of rhodes grass biochar is higher (16.78 m² g⁻¹) compared to date palm biochar (1.99 m² g⁻¹). This is in agreement with scanning electron microscopy investigations (SEM) which show that the average pore size diameter is smaller in rhodes grass biochar (3.1 μm + 0.3 μm) compared to the one of date palm biochar (7.2 μm ± 2.9 μm). Changes in the distribution of pore size diameter in the two biomass before and after pyrolysis suggests date palm is relatively heat sensitive in comparison to rhodes grass. Overall, our results demonstrate that both biochars are substantially different despite being produced under the same pyrolysis condition.

© 2014 Elsevier B.V. All rights reserved.

1. Introduction

Biochar is charcoal produced from organic materials – usually plant biomass – by means of pyrolysis. It is a porous inert form of carbon with low bulk density and high cation exchange capacity [1]. Because of these characteristics, the application of biochar to

soil has been demonstrated to improve certain properties such as nutrient adsorption, structure and water retention [1,2]. Indeed, the historic use of biochar can be traced back to 2000 years ago when ancient civilizations indigenous to the Amazon basin used it as a practice to enrich soil fertility [3]. Furthermore, some of the most fertile soils in the world contain natural deposits of biochar resulting from forest or grassland fires [4,5]. Biochar is also being considered as an inexpensive sustainable option for long term carbon storage in soils [6] as some studies demonstrated that the mean residence time of biochar can be greater than 1000 years [7,8].

Pyrolysis of biomass also yields gas and bio-oil as co-products alongside biochar. The fraction of each that is produced depends

* Corresponding authors at: Masdar Institute of Science and Technology, PO Box 54424, Abu Dhabi, United Arab Emirates. Tel.: +971 28109175.

E-mail addresses: mjouiad@masdar.ac.ae (M. Jouiad), lyousef@masdar.ac.ae (L.F. Yousef).

on the pyrolysis process, but slow heating rates ($<30^{\circ}\text{C min}^{-1}$) are recommended when biochar is the main product desired [9–11]. Furthermore, pyrolysis temperatures above 250°C are recommended for conversion of lignocellulosic biomass because decomposition of hemi-cellulose and cellulose begins at 250°C and is maximal at 400°C [12,13], whereas changes in lignin structure only start to occur after heating for long durations ($>8\text{ h}$) [12]. Clearly then, the conditions used to produce biochars are related to the type of biomass and pyrolysis conditions. Variability in these parameters ultimately results in different physicochemical properties of the biochars and affects their performance and utility for soil and other applications [14]. For this reason, many studies have been directed toward determining suitable sources of biomass [11,15] as well as optimizing pyrolysis conditions [9,17,18]. The challenge is to be able to predict quality and performance of biochars produced from a given biomass and a given pyrolysis process via analysis of its physicochemical properties.

In this study, two types of lignocellulosic biomass – fronds of date palm (*Phoenix dactylifera*) and rhodes grass (*Chloris gayana*) – were converted to biochar using the same condition of slow pyrolysis (1 atm; heating $5^{\circ}\text{C min}^{-1}$ up to 400°C ; duration of 11 h) and subsequently compared in terms of chemical composition, thermal stability, and microstructures. The motivation to explore these two biomass is related to environmental issues surrounding their cultivation in the United Arab Emirates (UAE). Palm tree cultivation in the UAE results in a large amount of lignocellulosic waste, (approximately 20 kg per tree annually) [19] that is transported to landfills. Achieving the conversion of palm tree waste to biochar may have a useful application in soil while providing a solution for waste management. Rhodes grass is valued among farmers because of the relative ease in setting the seed, and its tolerance to drought and soil salinity [20,21]. However, its cultivation in the sandy soils of the UAE is water-intensive ($15,700\text{ m}^3\text{ ha}^{-1}\text{ year}^{-1}$) and not sustainable [22]. A plausible solution is to improve the water holding capacity of the soils through the use of biochar soil amendment [23] by converting some of the rhodes grass harvest to biochar on-site and re-application to soil. The current study focuses on comparing the properties of the two biomass before and after their pyrolysis to biochar as basis for future studies involving their application to soil.

2. Materials and methods

2.1. Feedstock and biochars

Feedstock (rhodes grass and fronds of date palm) were obtained from a farm located in Sweihan, United Arab Emirates, air-dried for 72 h, oven dried at 100°C for 24 h then milled into pieces of approximately 2 mm prior to charring at atmospheric pressure in an electrically heated CrNiMoTi vessel reactor (Versoclave type 3E/2L, Buchiglauster Switzerland) using a heating rate of $5^{\circ}\text{C min}^{-1}$ up to 400°C and maintained at this temperature for 11 h (Fig. 1). Pyrolysis conditions were chosen based on several studies where the maximal temperature of decomposition of hemi-cellulose and cellulose by slow pyrolysis was reported to occur at 400°C [12,13], and changes in lignin structure only start to occur after heating for long durations [12], whereas a heating rate of $5^{\circ}\text{C min}^{-1}$ was selected as it has been commonly used for biochar production elsewhere [24–26].

2.2. Chemical composition, FTIR, and pH

Unless specified, all analyses were conducted in duplicate. TGA performed on an SDT Q600 (TA Instruments, New Castle, DE, USA) was used for proximate analysis [27]. A heating rate of $10^{\circ}\text{C min}^{-1}$

was used, first in an inert (nitrogen) atmosphere up to 700°C (for moisture and volatile determination) followed by a switch to a reactive (oxygen) atmosphere up to 1300°C (fixed carbon determination) (Supplementary Fig. S1). Ultimate composition analysis (CHNS) was determined on a dry weight basis using a Flash 2000 series elemental analyzer (Perkin Elmers, Watham, MA, USA). The oxygen content was determined on a dry weight basis by taking the difference ($\text{O}\% = 100 - \text{ash}\% - \text{C}\% - \text{N}\% - \text{H}\%$) [28]. Elemental analysis was used to calculate atomic molar ratios: H/C , O/C and $(\text{O} + \text{N})/\text{C}$ and $(\text{O} + \text{N} + \text{S})/\text{C}$. FTIR spectroscopy was performed using a Vertex 80v spectrophotometer (Bruker Corporation, Billerica, MA, USA) equipped with a diamond–platinum attenuated total reflectance (ATR), scanning in the range of $4000\text{--}400\text{ cm}^{-1}$ regions and having a spectral resolution of 4 cm^{-1} . Functional group identification from FTIR spectra was completed using data compiled from literature [12,29,30]. The pH of raw material and biochars were measured in milliQ water from a 1% (w/v) suspension after shaking at 150 rpm over 24 h at 25°C [28].

2.3. Thermal stability

Thermal stability experiments were performed using TGA on an SDT Q600 (TA Instruments, New Castle, DE, USA) using a heating rate of $10^{\circ}\text{C min}^{-1}$ to a final temperature of 1000°C in inert gas (nitrogen) atmosphere (Supplementary Fig. S2). The temperature at which maximum weight loss occurred was determined from the 1st derivative of weight loss from TGA curves. The data was then used to generate Table 2 and is representative of the thermal degradation of lignocellulosic biomass [12,18,31] – mainly the de-polymerization/volatilization of hemicellulose ($220\text{--}315^{\circ}\text{C}$), cellulose ($250\text{--}400^{\circ}\text{C}$) and lignin ($160\text{--}900^{\circ}\text{C}$) which occurs over several stages depending on the complexity of the biomass.

2.4. Microstructure analysis and water sorption

Surface area measurements were determined as multipoint Brunauer–Emmet–Teller (BET) obtained from N_2 adsorption isotherms at 77 K using Nova 2000e (Quantachrome Instruments, Boynton Beach, FL, USA). Water sorption experiments were performed on a VTI-SA Analyzer (TA Instruments, New Castle, DE, USA) – controlled relative humidity (RH%) was applied to dry samples and weight changes were measured gravimetrically. SEM observations were conducted at the Electron Microscopy Facility of Masdar Institute (Abu Dhabi, UAE) using a Quanta 250 SEM (FEI Company, Hillsboro, OR, USA). All samples were first quenched in liquid nitrogen for 5 min, cleaved and coated with fine film (5 nm) of gold palladium using PECS coating machine (Gatan Inc., Pleasanton, CA, USA) prior to imaging to reduce charging effects. SEM micrographs were processed and enhanced using Image J free-ware (<http://imagej.nih.gov/ij/>) for quantitative measurement of pore size distribution (Supplementary Fig. S3).

3. Results

3.1. Composition analysis and pH

Proximate composition analysis of the raw materials and resulting biochars are presented in Table 1. Conversion of raw biomass to biochars resulted in higher contents of fixed carbon and ash, and lower contents of moisture and volatiles (Table 1). Comparison of the two biochars revealed that rhodes grass biochar has a higher content of fixed carbon, but lower contents of volatiles and moisture (56.6%, 11.8% and 1.8% wet wt. respectively) compared to date palm (45% and 43.2% and 4.8% wet wt., respectively). However, the

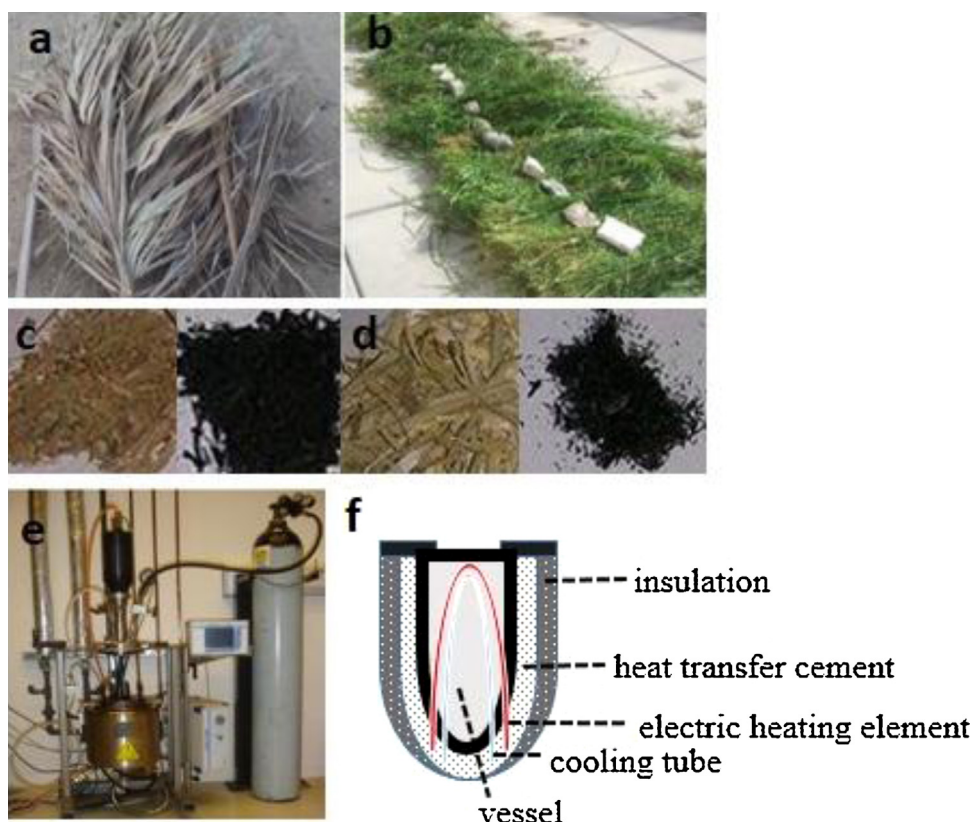


Fig. 1. Raw biomass, biochars and reactor used. (a) Air-dried fronds of date palm, (b) air-dried rhodes grass, (c) milled palm fronds (left) and resulting biochar (right), (d) milled rhodes grass (left) and resulting biochar (right), (e) Buchiglauster electrically heated reactor used in this study and (f) 1D cartoon profile showing elements of the reactor.

ash content in rhodes grass biochar is higher (28.8% wet wt.) compared to date palm biochar (7.1% wet wt.). The pH of both date palm and rhodes grass became more alkaline after conversion to biochar (Table 1), with rhodes grass biochar exhibiting a slightly higher pH (9.7) compared to date palm biochar (9.5).

Elemental analysis (Table 1) showed pyrolysis enriched carbon and depleted hydrogen, oxygen and sulfur. Nitrogen composition did not change after pyrolysis in rhodes grass (1.9% dry wt.), but it

increased in date palm from below detection limit to 1.2% dry wt. The atomic molar ratios for H/C and O/C, (O + N)/C and (O + N + S)/C (Table 1) all decreased after pyrolysis. Date palm and rhodes grass biochars have similar molar ratios for H/C (0.49 and 0.46 respectively), but date palm biochar has a three-fold higher molar ratio for O/C, (O + N)/C and (O + N + S)/C compared to rhodes grass biochar (Table 1).

3.2. Thermal stability

Thermal degradation events for rhodes grass and date palm are presented in Table 2 according to weight loss resulting from decomposition of hemi-cellulose, cellulose and lignin (see materials and methods). Biochars underwent a fewer number of thermal decomposition events when compared to raw biomass. Comparative analysis of the two biochars reveals considerable differences. First, weight loss for rhodes grass biochar occurred slowly but continuously over a single, but wide temperature range (120–1000 °C; no obvious degradation maximum). In contrast, weight loss for date palm biochar occurred over two decomposition events – the first occurred rapidly over a narrow temperature range (280–380 °C; maximum at 340 °C) and the second event occurred slowly over a wider temperature range (380–1000 °C; no temperature maximum detected) (Table 2). Furthermore, total weight loss (excluding moisture) resulting from thermal degradation was drastically lower in rhodes grass biochar (12 wt%) than in date palm biochar (43 wt%).

3.3. Surface functional groups

The FTIR spectra of the raw biomass and biochars is shown in Fig. 2. Overall, the FTIR spectral features are generally lost

Table 1
Characteristics of raw biomass and biochars.

Characteristics	Raw		Biochar	
	Date palm	Rhodes grass	Date palm	Rhodes grass
pH	5.9	6.1	9.5	9.7
BET surface area (m ² g ⁻¹)	0.98	1.97	1.99	16.78
Moisture (%)	6.2	7.8	4.8	1.8
Proximate analysis, ^a (%)				
Volatiles	69.9	66.5	43.2	11.8
Fixed carbon	20.9	11.0	45.0	56.6
Ash	2.9	14.7	7.1	28.8
Ultimate analysis, ^b (%)				
Carbon	45.4	42.5	60.9	56.7
Hydrogen	5.6	5.5	2.5	2.2
Oxygen	40.4	28.7	25.6	8.2
Sulfur	5.5	5.3	2.2	1.6
Nitrogen	0	1.9	1.2	1.9
Molar ratio				
H/C	1.47	1.54	0.49	0.46
O/C	0.67	0.51	0.32	0.11
(O + N)/C	0.67	0.55	0.33	0.14
(O + N + S)/C	0.71	0.59	0.35	0.15

^a Weight percentage on wet basis.

^b Weight percentage on dry basis.

Table 2

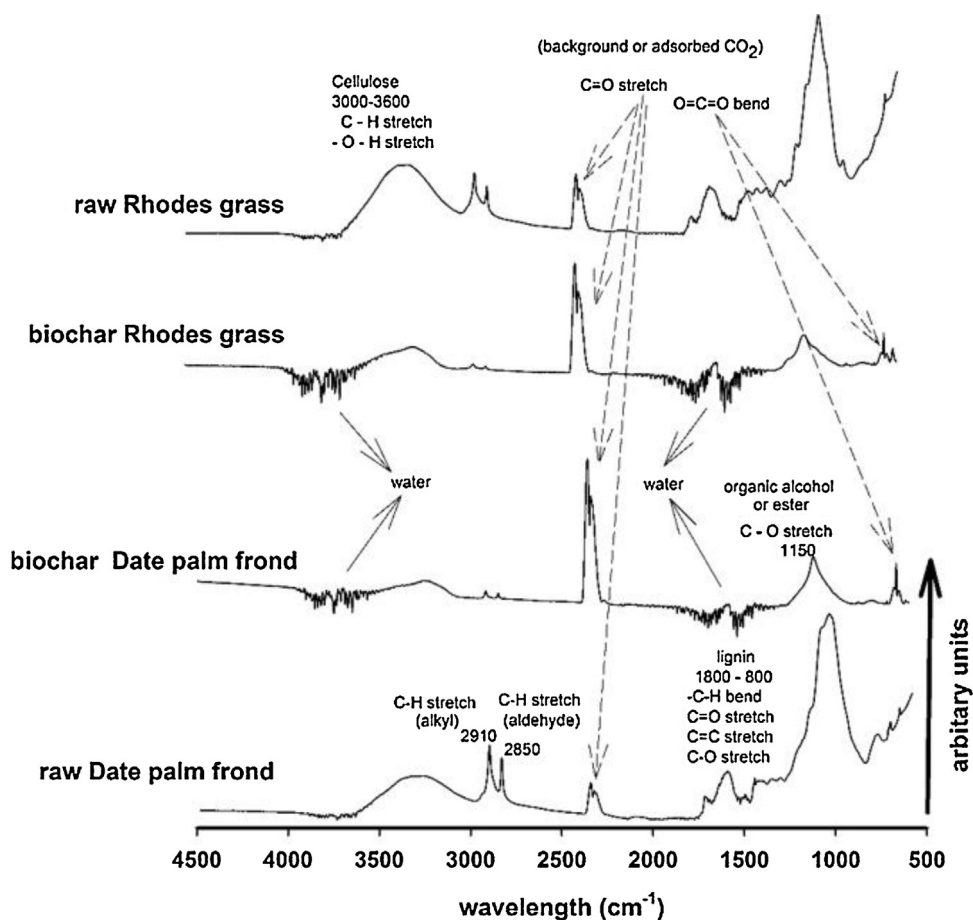
Thermal decomposition of raw biomass and biochars in an inert gas atmosphere.

Biomass component	Raw		Biochar	
	Date palm	Rhodes grass	Date palm	Rhodes grass
Hemicellulose				
Mass loss (%)	22.95	20.59	–	–
Degradation range (°C)	120–280	120–280	–	–
Degradation maximum (°C)	250	270	–	–
Cellulose				
Mass loss (%)	31.27	20.71	21.80	–
Degradation range (°C)	280–380	280–380	280–380	–
Degradation maximum (°C)	320	320	340	–
Lignin				
Mass loss (%)	15.63	25.18	21.80	11.77
Degradation range (°C)	380–1000	380–1000	380–1000	120–1000
Degradation maximum (°C)	n/a	n/a	n/a	n/a

n/a = temperature maximum not detected. (–) = absence of event.

in the biochars when compared to raw biomass. The bands assigned to O–H stretching ($3200\text{--}3000\text{ cm}^{-1}$) and C–H stretching ($3100\text{--}3000\text{ cm}^{-1}$) are attributed to hemicellulose and cellulose, which markedly decrease in both biochars (Fig. 2). This suggests that structural changes occurred during pyrolysis, such as a decrease in aliphatic compounds. Moreover, the presence of asymmetric (2910 cm^{-1}) and symmetric (2850 cm^{-1}) C–H stretching bands also associated with aliphatic functional groups, are stronger in the raw materials when compared to biochars. Bands associated with carboxylic groups (C=O) (e.g. ketones, esters, carboxyl) were detected in the spectra of raw material (Fig. 2) but not in the spectra of biochars. The source of these functional groups

is most likely hemi-cellulose, which is also supported with the absence of a thermal decomposition event associated with hemicellulose in the biochars (Table 2). Bands associated with aromatic C=C stretching and C=O associated with ketones or Quinones ($1600\text{--}1580\text{ cm}^{-1}$) were also drastically reduced in the biochars. Bands in the $900\text{--}1400\text{ cm}^{-1}$ region are representative of lignin, mostly because of C=C ring stretching. A weak band at 1150 cm^{-1} in both biochars are assigned to C–O stretch from organic alcohols or esters. Interestingly, bands characteristic for CO₂ are present in the spectra of both biochars (Fig. 1). Bands in the $4000\text{--}3500\text{ cm}^{-1}$ and $2000\text{--}1200\text{ cm}^{-1}$ regions present in both biochars spectra are characteristic of water.

**Fig. 2.** FTIR spectra of raw biomass and resulting biochars after pyrolysis.

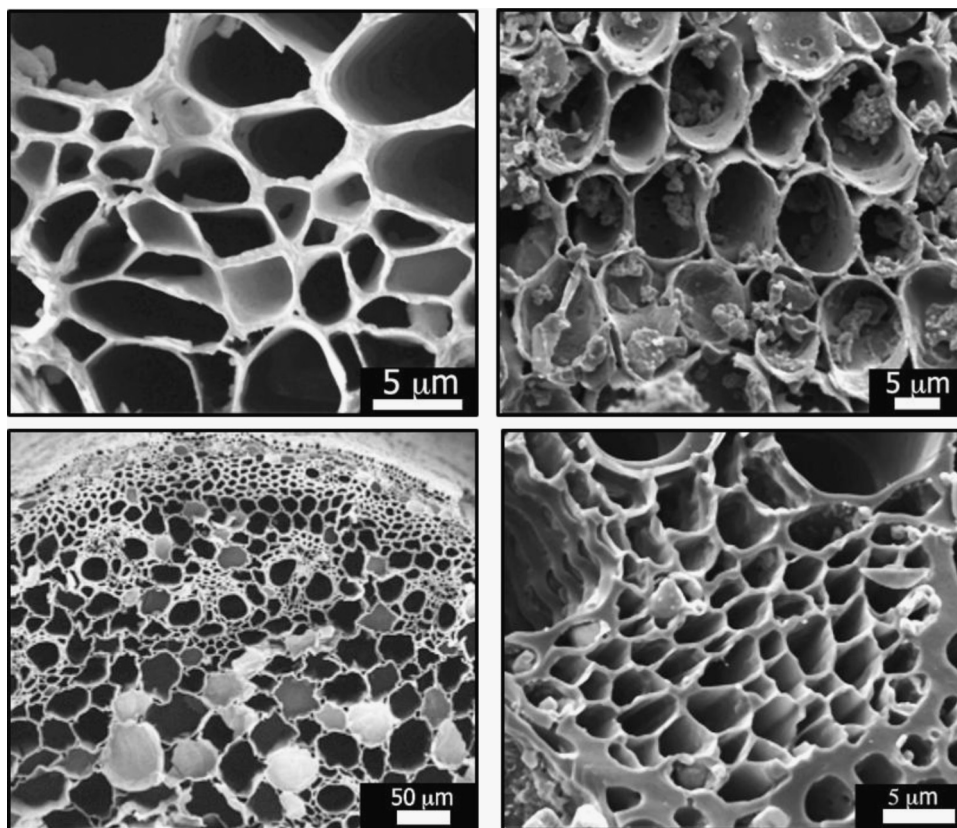


Fig. 3. Secondary electron imaging of raw date palm (top left), date palm biochar (top right), raw rhodes grass (bottom left) and rhodes grass biochar (bottom right).

3.4. Surface area, microstructure analysis and water sorption

Conversion of raw material to biochar increased the BET surface area (Table 1), but rhodes grass biochar has a higher BET surface

area ($16.78 \text{ m}^2 \text{ g}^{-1}$) compared to date palm biochar ($1.99 \text{ m}^2 \text{ g}^{-1}$). Microstructure analyses of the materials using SEM are shown in Fig. 3. It shows that macropores ($>50 \text{ nm}$) with different shapes, morphologies and sizes are present in raw and biochar materials

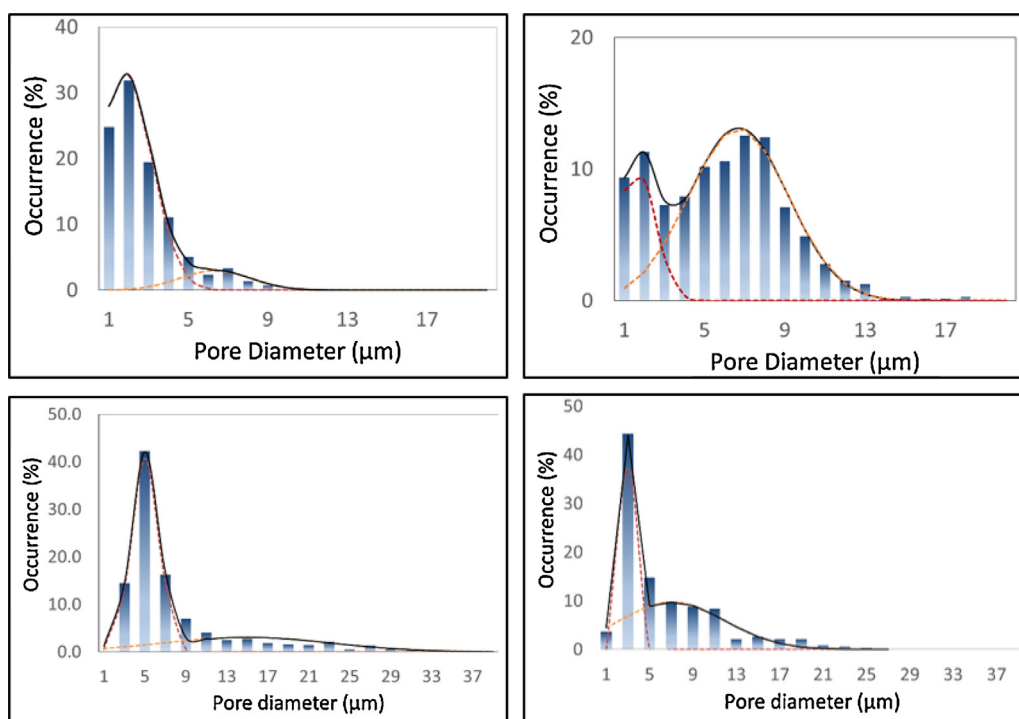


Fig. 4. Pore size distribution (bars) and normal distribution fitting (dashed and full lines) for raw date palm (top left), date palm biochar (top right), raw rhodes grass (bottom left) and rhodes grass biochar (bottom right).

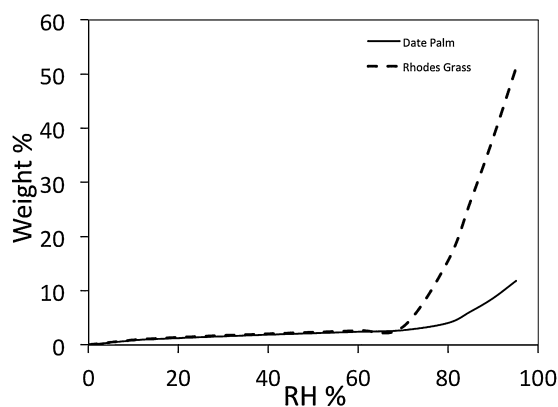


Fig. 5. Water vapor sorption analysis for date palm and rhodes grass biochars.

(Fig. 3). Conversion of raw date palm to biochar appears to enlarge pores and make them more uniform in shape. In contrast, conversion of rhodes grass to biochar appears to shrink pores and make them more heterogeneous in shape. Image J software analysis of the SEM micrographs (Supplementary Fig. S3) was then used to take a more quantitative approach by measuring pore sizes in the materials and plot their distribution (Fig. 4). In raw date palm, two normal-shaped distributions for pore size are found – a dominant distribution for small pores ($2.8 \mu\text{m} \pm 1.9 \mu\text{m}$) and a secondary distribution for larger pores ($7.3 \mu\text{m} \pm 2.5 \mu\text{m}$) (Fig. 4 upper left image). Conversion of raw date palm to biochar caused an enlargement in pore size because the dominant distribution is for larger pores ($7.2 \mu\text{m} \pm 2.9 \mu\text{m}$) compared to smaller pores ($2.6 \mu\text{m} \pm 1.3 \mu\text{m}$) (Fig. 4 upper right image). In comparison, pore size distributions in rhodes grass before and after pyrolysis have the same shape (Fig. 4 bottom images); a major peak followed by a relatively small and broad one. Also, the first peak mean size, considering the measurement errors are slightly similar: ($5 \mu\text{m} \pm 1.4 \mu\text{m}$) and ($3.1 \mu\text{m} \pm 0.3 \mu\text{m}$) for raw and biochar forms of rhodes grass. Overall, the results from pore size suggest that date palm structure is temperature sensitive and exhibits a noticeable instability to pyrolysis in comparison to rhodes grass. The adsorption of water vapor at controlled relative humidity (RH%) for date palm and rhodes grass biochars is shown in Fig. 5. Both biochars show slow water uptake up to 70% RH after which there is a rapid increase in water uptake in rhodes grass and date palm respectively.

4. Discussion

It is well known that biochar quality varies according to biomass and pyrolysis conditions used [10,11,28] but also the assessment of quality is a rather abstract process. The International Biochar Initiative (IBI) considers several parameters relevant for assessing and comparing different biochars [33]. These include proximate analysis, elemental composition analysis, pH, porosity and BET surface area. In this study, two types of biomass (rhodes grass and fronds of edible date palm) were converted to biochar using the same pyrolysis condition (1 atm; heating 5°C min^{-1} up to 400°C ; 11 h duration) and then assessed and compared in terms of chemical composition, thermal stability, and microstructures.

Generally, biochars with high fixed carbon, low volatile matter and ash are more economically attractive if they are to be purchased for use in long-term carbon sequestration in soil [34,35]. Fixed carbon being indicative of recalcitrant carbon that is resistant to biological decomposition – hence high values are favorable [35]. High values of ash and volatiles in biochar are unfavorable because they provide little long-term value, and evidence suggests that volatile matter leaching into soil presents microbes with a labile

form of carbon allowing them to compete with plants for nutrients [36]. However, the dissolution of volatiles/organics in water is dictated by their physical properties and hydrophobicity – therefore volatile losses as leachate may not always occur. In this study, rhodes grass biochar has higher fixed carbon (56.6% vs. 45% wt. in date palm) and lower volatile matter (11.8% vs. 45% wt. in date palm) compared to date palm biochar. The only caveat being rhodes grass biochar having higher ash than date palm biochar (28.8% vs. 7.1% wt.). However, the ash content in rhodes grass is in the acceptable range of biochars produced from non woody material for soil amendment [10]. Overall, rhodes grass appears to be better than date palm biochar when using proximate analysis as a proxy for biochar quality.

In addition to proximate analysis, atomic H/C and O/C ratios are often used as indicators of carbonization and biochar stability against decomposition [7,34,35]. Biochars with O/C ratios below 0.2 are predicted to have a half-life of at least 1000 years [7]. The O/C and (O + N)/C ratios are also often used to reflect on the relative hydrophobicity of biochar (i.e. likelihood of interacting with water) [28,37,38]. In this study, the atomic ratios were calculated (Table 1) after elemental analysis. We find that pyrolysis of raw biomass to biochars enriched carbon, and depleted oxygen, hydrogen and sulfur content – which is the typical response to biomass pyrolysis (e.g. [11]). However, nitrogen appears to be stable in the biomass because it did not change after pyrolysis in rhodes grass and even increased in date palm from below detection limit to 1.2% (Table 1). Relative increases in N content with increasing pyrolysis temperature (200–800 °C) has been reported in another biochar study involving *Conocarpus* (type of mangrove) waste [18]. The calculated atomic H/C ratios are similar in the two biochars (ca. 0.5) (Table 1) suggesting that the two biomass underwent similar degrees of carbonization during pyrolysis [35]. However, the two biochars differed in their atomic O/C and (O + N)/C ratios (Table 1) – both ratios were three-fold higher in date palm (ca. 0.3) compared to rhodes grass (ca. 0.1). This data suggests that rhodes grass is relatively more hydrophobic when compared to date palm biochar, and probably more stable against decomposition [38].

Thermal degradation profiles were different for the two biochars in this study (Table 2). Total weight loss (excluding moisture) resulting from thermal decomposition events was drastically lower in rhodes grass biochar (ca. 12 wt%) compared to date palm biochar (ca. 43 wt%). An event (maximum at 340°C) attributed to cellulose was observed in date palm biochar, but not in rhodes grass biochar (Table 2). In rhodes grass biochar – a single event that occurred over a broad temperature was attributed to lignin because the material is known to decompose over a range of $160\text{--}900^\circ\text{C}$ [13,32]. However, FTIR analysis (Fig. 2) shows that cellulose was still present in both biochars. Therefore, some of the weight loss that we attributed to lignin in rhodes grass maybe a result of cellulose decomposition.

Several other studies characterized biochar produced from oil palm kernel shells [19], date palm seeds [39] and date palm fronds [40] using a range of conversion methods, but to our knowledge studies on biochar produced from rhodes grass are not available. The conditions used to generate biochar from palm biomass in other studies were different from conditions used in this study. For example, one biochar was produced from oil palm fronds in a muffle furnace after burning 320°C for 4 h [41]. The study reported similar pH values to our study (Table 1), and cellulose in their study was not completely disintegrated, similar to our findings from FTIR analysis (Fig. 2). However, they also reported higher BET values ($9 \text{ m}^2 \text{ g}^{-1}$) [41] than what we report in this study for palm ($1.99 \text{ m}^2 \text{ g}^{-1}$) (Table 1). Pyrolysis temperature has been shown to affect BET surface area – it increases if temperatures of $500\text{--}700^\circ\text{C}$ are used [9]. Increases in surface area of biochars is a result organic volatilizations lost from biomass during pyrolysis, which create voids within the material thereby increasing porosity and total

surface area. However, the condensation of organic volatiles after pyrolysis may also clog pores and result in lower BET surface areas than expected. We therefore suspect that the higher volatile content in date palm (Table 1) may be responsible for the relatively low BET surface area measured in the date palm biochar (Table 1). SEM images taken of the date palm biochar seem to support this hypothesis (Fig. 3 upper right) – it shows condensate like residue that appear to clog the pores.

Lastly, we were interested in biochar pore size distribution because the information may be useful for applications that aim to improve water holding capacity of sandy soils through textural conditioning [23]. We conducted two types of analysis – the first was a quantitative measurement of pore size diameter using SEM images (Fig. 4), and the second was a water sorption analysis of the materials (Fig. 5). SEM image analysis of the two biomass showed that pyrolysis of rhodes grass induced little changes to pore size (average pore size ca. 3 μm) whereas it caused an enlargement in pore diameter in date palm (from ca. 3 to 7 μm) (Fig. 4). Despite the different pore size observed in the biochars, both pore sizes would be classified as macropores ($>0.05 \mu\text{m}$ or 50 nm pore size) according to International Union of Pure and Applied Chemistry [42]. Indeed, water sorption analysis of the biochars (Fig. 5) indicated they behave as macroporous materials. As described elsewhere, the diameter of a water molecule is 0.28–0.3 nm [43]. Therefore, water first fills micropores and mesopores by physisorption processes [44] and then water is adsorbed into the surface of pore walls and condenses to fill the core of the macropores [45]. Hence, at low RH, water fills the smallest pores first in the biochars and then water adsorbs in layers to their surface. The low uptake of water at low RH (Fig. 5) suggests that both biochars behave as macroporous materials [45] because only negligible water uptake was observed at the first stages of water adsorption rhodes grass and date palm biochars have similar water sorption behavior, but there was a more rapid uptake of water measured in rhodes grass past 70% RH (Fig. 5) suggesting it has smaller sized pores in comparison to date palm biochar. Using this information, we predict that both biochars may have similar potential for improving water holding capacity of soils. However, differences in hydrophobicity of the two biochars (discussed earlier) may play a role in retention and bioavailability of water.

On a final note, FTIR analysis (Fig. 2) showed strong bands characteristic for CO_2 are present in the spectra of both biochars [30]. This could be indicative of biochar's sorptive properties for atmospheric CO_2 . One study reported that biochar mixed into soil was effective at reducing atmospheric CO_2 concentrations, and biochar is being proposed for utility in highly polluted regions for CO_2 reduction [46]. Therefore, the biochars used in this study may potentially be used in a similar application, but this will require additional research.

5. Conclusions

Biomass composition plays an important role in the resulting properties of biochar. As demonstrated in this study, two types of biomass (rhodes grass and fronds of date palm) were characterized and compared after their slow pyrolysis to biochar using the same condition. Using proximate analysis and atomic ratios (H/C, O/C and O+N/C) as proxies for biochar assessment/quality – we predict rhodes grass biochar to be more stable and relatively more hydrophobic compared to date palm biochar. Rhodes grass biochar also exhibited higher stability to thermal degradation in comparison to date palm biochar. From these analysis, rhodes grass biochar appears to be more suitable for carbon sequestration type of applications. Macropores in the size range of 2–7 μm are dominant in both biochars suggesting they have similar capacities

for water retention related applications. Future research will be directed toward linking biochar properties from this study to soil benefits or other environmental applications.

Acknowledgements

This study was funded by a seed grant provided by the Masdar Institute of Science and Technology (Lina F Yousef). We thank Elena Guillen (iWATER, MIST) and Cyril Aubry (Office of Research, MIST) for analytical support.

Appendix A. Supplementary data

Supplementary data associated with this article can be found, in the online version, at <http://dx.doi.org/10.1016/j.jaap.2014.10.024>.

References

- [1] L. Beesley, E. Moreno-Jiménez, J.L. Gomez-Eyles, E. Harris, B. Robinson, T. Sizmur, A review of biochars' potential role in the remediation, revegetation and restoration of contaminated soils, *Environ. Pollut.* 159 (2011) 3269–3282.
- [2] S.P. Sohi, E. Krull, E. Lopez-Capel, R. Bol, Chapter 2 – a review of biochar and its use and function in soil, *Adv. Agron.* 105 (2010) 47–82.
- [3] E.H. Novotny, M.H.B. Hayes, B.E. Madari, T.J. Bonagamba, E.R.de. Azevedo, A.A. de Souza, G. Song, C.M. Nogueira, A.S. Mangrich, Lessons from the Terra Preta de Índios of the Amazon region for the utilisation of charcoal for soil amendment, *J. Braz. Chem. Soc.* 20 (2009) 1003–1010.
- [4] T.H. DeLuca, M.D. MacKenzie, M.J. Gundale, W.E. Holben, Wildfire-produced charcoal directly influences nitrogen cycling in ponderosa pine forests, *Soil Sci. Soc. Am. J.* 70 (2006) 448.
- [5] J.O. Skjemstad, D.C. Reicosky, A.R. Wilts, J.A. McGowan, Charcoal carbon in U.S. agricultural soils, *Soil Sci. Soc. Am. J.* 66 (2002) 1249.
- [6] D. Woolf, J.E. Amonette, F.A. Street-Perrott, J. Lehmann, S. Joseph, Sustainable biochar to mitigate global climate change, *Nat. Commun.* 1 (2010) 56.
- [7] K.A. Spokas, Review of the stability of biochar in soils: predictability of O:C molar ratios, *Carbon Manag.* 1 (2010) 289–303.
- [8] B.P. Singh, A.L. Cowie, R.J. Smernik, Biochar carbon stability in a clayey soil as a function of feedstock and pyrolysis temperature, *Environ. Sci. Technol.* 46 (2012) 11770–11778.
- [9] O. Mašek, P. Brownsort, A. Cross, S. Sohi, Influence of production conditions on the yield and environmental stability of biochar, *Fuel* 103 (2013) 151–155.
- [10] F. Ronsse, S. van Hecke, D. Dickinson, W. Prins, Production and characterization of slow pyrolysis biochar: influence of feedstock type and pyrolysis conditions, *GCB Bioenergy* 5 (2013) 104–115.
- [11] S. Kloss, F. Zehetner, A. Dellantonio, R. Hamid, F. Ottner, V. Liedtke, M. Schwanninger, M.H. Gerzabek, G. Soja, Characterization of slow pyrolysis biochars: effects of feedstocks and pyrolysis temperature on biochar properties, *J. Environ. Qual.* 41 (2012) 990–1000.
- [12] D.W. Rutherford, R.L. Wershaw, C.E. Rostad, C.N. Kelly, Effect of formation conditions on biochars: compositional and structural properties of cellulose, lignin, and pine biochars, *Biomass Bioenergy* 46 (2012) 693–701.
- [13] P.T. Williams, S. Besler, The influence of temperature and heating rate on the slow pyrolysis of biomass, *Renew. Energy* 7 (1996) 233–250.
- [14] C.E. Brewer, R. Unger, K. Schmidt-Rohr, R.C. Brown, Criteria to select biochars for field studies based on biochar chemical properties, *BioEnergy Res.* 4 (2011) 312–323.
- [15] D. Özçimen, A. Ersoy-Meriçboyu, Characterization of biochar and bio-oil samples obtained from carbonization of various biomass materials, *Renew. Energy* 35 (2010) 1319–1324.
- [17] T. Imam, S. Capareda, Characterization of bio-oil, syn-gas and bio-char from switchgrass pyrolysis at various temperatures, *J. Anal. Appl. Pyrolysis* 93 (2012) 170–177.
- [18] M.I. Al-Wabel, A. Al-Omran, A.H. El-Naggar, M. Nadeem, A.R.A. Usman, Pyrolysis temperature induced changes in characteristics and chemical composition of biochar produced from conocarpus wastes, *Bioresour. Technol.* 131 (2013) 374–379.
- [19] M. Chandrasekaran, A.H. Bahkali, Valorization of date palm (*Phoenix dactylifera*) fruit processing by-products and wastes using bioprocess technology—review, *Saudi J. Biol. Sci.* 20 (2013) 105–120.
- [20] A.E. Eneji, S. Inanaga, S. Muranaka, J. Li, T. Hattori, P. An, W. Tsuji, Growth and nutrient use in four grasses under drought stress as mediated by silicon fertilizers, *J. Plant Nutr.* 31 (2008) 355–365.
- [21] A.E. Osman, M. Makawi, R. Ahmed, Potential of the indigenous desert grasses of the Arabian Peninsula for forage production in a water-scarce region, *Grass Forage Sci.* 63 (2008) 495–503.
- [22] N.K. Rao, M. Shahid, Potential of cowpea [*Vigna unguiculata* (L.)] and guar [*Cyamopsis tetragonoloba* (L.) Taub.] as alternative forage legumes in the United Arab Emirates, *Emirates J. Food Agric.* 23 (2011) 147–156.

- [23] A.S. Basso, F.E. Miguez, D.A. Laird, R. Horton, M. Westgate, Assessing potential of biochar for increasing water-holding capacity of sandy soils, *GCB Bioenergy* 5 (2013) 132–143.
- [24] L. Van Zwieten, S. Kimber, S. Morris, K.Y. Chan, A. Downie, J. Rust, S. Joseph, A. Cowie, Effects of biochar from slow pyrolysis of papermill waste on agronomic performance and soil fertility, *Plant Soil* 327 (2009) 235–246.
- [25] F. Karaosmanolu, A. Işığür-Ergüdenler, A. Sever, Biochar from the straw-stalk of rapeseed plant, *Energy Fuels* 14 (2000) 336–339.
- [26] N.M. Noor, A. Shariff, N. Abdullah, Slow pyrolysis of cassava wastes for biochar production and characterization, *Iran. J. Energy Environ.* 3 (2012) 60–65.
- [27] M.C. Mayoral, M.T. Izquierdo, J.M. Andrés, B. Rubio, Different approaches to proximate analysis by thermogravimetry analysis, *Thermochim. Acta* 370 (2001) 91–97.
- [28] J. Novak, I. Lima, B. Xing, J. Gaskin, C. Steiner, K. Das, M. Ahmedna, D. Rehrh, D. Watts, W. Busscher, et al., Characterization of designer biochar produced at different temperatures and their effects on a loamy sand, *Ann. Environ. Sci.* 3 (2009) 195–206.
- [29] W. Wu, M. Yang, Q. Feng, K. McGrouther, H. Wang, H. Lu, Y. Chen, Chemical characterization of rice straw-derived biochar for soil amendment, *Biomass Bioenergy* 47 (2012) 268–276.
- [30] R.M. Silverstein, F.X. Webster, *Infrared spectrometry Spectrometric Identification of Organic Compounds*, vol. 39, Wiley, 1996, pp. 71–143.
- [31] L. Gašparovič, Z. Koreňová, L. Jelemenský, Kinetic study of wood chips decomposition by TGA, *Chem. Pap.* 64 (2009) 174–181.
- [32] H. Yang, R. Yan, H. Chen, D.H. Lee, C. Zheng, Characteristics of hemicellulose, cellulose and lignin pyrolysis, *Fuel* 86 (2007) 1781–1788.
- [33] IBI, Biochar Initiative (IBI) Guidelines for Specifications of Biochars for Use in Soils, 2012, Westerville, OH.
- [34] A.R. Zimmerman, Abiotic and microbial oxidation of laboratory-produced black carbon (biochar), *Environ. Sci. Technol.* 44 (2010) 1295–1301.
- [35] A. Enders, K. Hanley, T. Whitman, S. Joseph, J. Lehmann, Characterization of biochars to evaluate recalcitrance and agronomic performance, *Bioresour. Technol.* 114 (2012) 644–653.
- [36] J. Deenik, Charcoal effects on soil properties and plant growth: charcoal ash and volatile matter effects on soil properties and plant growth in an acid ultisol, *Soil Sci.* 176 (2011) 336–345.
- [37] X. Wang, R. Cook, S. Tao, B. Xing, Sorption of organic contaminants by biopolymers: role of polarity, structure and domain spatial arrangement, *Chemosphere* 66 (2007) 1476–1484.
- [38] K.A. Spokar, Review of the stability of biochar in soils: predictability of O:C molar ratios, *Carbon Manag.* 1 (2010) 289–303.
- [39] K.S.K. Reddy, A. Al Shoaibi, C. Srinivasakannan, Activated carbon from date palm seed: process optimization using response surface methodology, *Waste Biomass Valor.* 3 (2012) 149–156.
- [40] H.H. Sait, A. Hussain, A.A. Salema, F.N. Ani, Pyrolysis and combustion kinetics of date palm biomass using thermogravimetric analysis, *Bioresour. Technol.* 118 (2012) 382–389.
- [41] S.H. Kong, S.K. Loh, R.T. Bachmann, Y.M. Choo, J. Salimon, S.A. Rahim, Production and physico-chemical characterization of biochar from palm kernel shell, in: *The 2013 UKM FST Postgraduate Colloquium: Proceedings of the Universiti Kebangsaan Malaysia, Faculty of Science and Technology 2013 Postgraduate Colloquium*, vol. 1571, AIP Publishing, 2013, pp. 749–752.
- [42] K.S.W. Sing, D.H.R.A.H. Everett, L. Moscou, R.A. Pierotti, J. Rouquerol, T. Siemieniewska, Reporting physisorption data for gas/solid systems, *Pure Appl. Chem.* 57 (1985) 603–619.
- [43] S. Ozeki, Dielectric properties of water adsorbed in slitlike micropores of jarosite, *Langmuir* 5 (1989) 181–186.
- [44] K. Sing, S.W. Everett, H.D. Hall, R.A.W. Moscou, L. Pierotti, R.A. Rouquerol, J.T. T. Siemieniewska, Reporting Physisorption Data for Gas/Solid Systems with Special Reference to the Determination of Surface Area and Porosity, 57th ed., *Inter. Un. of Pure and Appl. Chem.*, 1997, pp. 603–619.
- [45] C. Aharoni, The solid–liquid interface in capillary condensation. Sorption of water by active carbons, *Langmuir* 13 (1997) 1270–1273.
- [46] P.R. Tayade, V.S. Sapkal, R.S. Sapkal, S.K. Deshmukh, C.V. Rode, V.M. Shinde, G.S. Kanade, A method to minimize the global warming and environmental pollution, *J. Environ. Sci. Eng.* 54 (2012) 287–293.